Layer interdependence of transport in an undoped electron-hole bilayer

Christian P. Morath,* John A. Seamons, John L. Reno, and Mike P. Lilly
Sandia National Laboratories, Albuquerque, New Mexico 87185, USA

(Received 7 March 2008; revised manuscript received 8 August 2008; published 23 September 2008)

The layer interdependence of transport in an undoped electron-hole bilayer (UEHBL) device was studied as a function of carrier density, interlayer electric field, and temperature. The UEHBL device consisted of a density tunable, independently contacted two-dimensional electron gas (2DEG) and two-dimensional hole gas (2DHG) in distinct (100) GaAs quantum wells separated by a 30 nm $Al_{0.9}Ga_{0.1}As$ barrier. The 2DEG and 2DHG are induced via field effect by top and bottom gates, respectively. Transport measurements were made simultaneously on each layer using the van der Pauw method. An increase in 2DHG mobility with increasing 2DEG density was observed, while the 2DEG mobility showed minimal dependence on the 2DHG density. Changes in both surface-gate voltages for the mobility-density measurements were observed. Decreasing the interlayer electric field and thereby increasing interlayer separation also increased the 2DHG mobility with negligible effects on the 2DEG mobility. The change in interlayer separation as interlayer electric field changed was estimated using 2DHG Coulomb drag measurements. A general discussion of the results is given in which the possible sources for the apparent interlayer dependence of the hole transport are examined.

DOI: 10.1103/PhysRevB.78.115318 PACS number(s): 73.63.Hs, 73.40.Rw, 73.40.Ty

I. INTRODUCTION

Interest in electron-hole bilayers necessarily arose from the prospect of observing Bose-Einstein condensation of excitons in semiconductor double quantum well systems[1,2] and significant progress toward this goal has been made.[3,4] This trend in bilayer research centered on the behavior of the electron-hole pair. The work presented in this paper, however, focuses on the individual transport in each layer and the layer interdependence. The latter is the primary question we seek to answer here and for which a bilayer device is singularly, exceptionally suited: to what extent will the mere presence of a nearby two-dimensional electron gas (2DEG) affect the transport in a two-dimensional hole gas (2DHG) and vice versa?

The general transport properties of the 2DEG system in modulation-doped heterostructures were well established decades ago.[5,6] Evidence for how the carrier mobility in these systems can be varied, via changes to scattering time or effective mass, will be emerged later. Exploiting Coulomb scattering's dependence on the shape of the wave function, Hirakawa *et al.*[7] demonstrated that a 2DEG's mobility could be altered by deforming the wave function using external fields from gates.[8,9] Calculations by Kurobe[10] also showed that the 2DEG wave function can be *squeezed* by changing surface-gate voltages; when the 2DEG's confining potential is tilted by an electric field, the wave function is squeezed against an interface. Furthermore, the calculations showed that this squeezing reduces remote and space impurity scattering times but enhances the channel impurity scattering time. From other studies on similar devices it was determined that background channel impurities dominate scattering at low densities, while interface roughness dominates at higher densities.[11,12] More recently, Das Sarma *et al.*[13] and Manfra *et al.*[14] showed that background impurity scattering in GaAs heterostructures is rudimentary to the two-dimensional (2D) metal-insulator transition, which occurs as density is reduced and screening of the random potential landscape, due to these impurities, becomes progressively weaker. Changes to the effective mass, a second possible mechanism to vary mobility, have also been recently investigated. Zu *et al.*[15] showed how a 2DHG effective mass varies with well parameters and density due to the highly nonparabolic valence subband structure. Lastly, several studies of spin-orbit coupling induced Rashba effect have shown that the spin splitting of the hole subband could be controlled via surface-gate voltages and how this changes the densities of the spin-split subbands.[16,17] These subbands have different effective mass, and thus, a change in the relative populations of each may influence mobility. These studies, however, were all on unipolar devices and an experimental study of whether general transport, specifically carrier mobility, is affected by a 2D system of opposite charge in close proximity has not been reported.

In this paper, the results of an investigation into the layer interdependence of transport in an undoped electron-hole bilayer (UEHBL) are presented. The UEHBL device under study consists of a density tunable, independently contacted 2DEG and 2DHG induced via field effect in distinct GaAs quantum wells separated by a 30 nm $Al_{0.9}Ga_{0.1}As$ barrier.[18] To populate the undoped wells an interlayer electric field E_{IL} is necessarily established to account for the energy difference between the conduction and valence bands. This design affords the following advantages: (1) independent contacts allow for simultaneous transport measurements of each layer and Coulomb drag measurements; (2) a tunable density 2DEG and 2DHG allows for these measurements to be made as functions of the density in each layer, n and p; (3) an undoped structure reduces scattering by remote ionized impurities; and (4) for equal densities, the interlayer separation d between the 2DEG and 2DHG can be varied by changing E_{IL} and both gate voltages. The investigation included mobility and resistivity measurements measured in each layer as functions of n and p, E_{IL}, and temperature T. Coulomb drag measurements were used to estimate the change in d as E_{IL} was varied.

The paper is organized as follows. An explanation of the device material and fabrication is given in Sec. II. Details regarding the device operation and experiment are presented in Sec. III. The results are presented in Sec. IV. They indicate that 2DHG transport changed by varying n or E_{IL}, while the transport observed in the 2DEG was largely immune to similar magnitude changes in p or E_{IL}. The apparent layer interdependence demonstrated by the 2DHG transport may only have been indirect; however, since increasing n also necessitated changes to the surface-gate voltage predominantly controlling p, which also would have affected the shape of the 2DHG confinement potential. Changes in confinement potential are known to affect 2DHG transport and whether any mechanisms are appropriate to the changes in hole mobility observed in the UEHBL is discussed in Sec. VI. This discussion is augmented with Coulomb drag measurements that were used to estimate the change in hole wave-function position with V_{IL}. Finally, in Sec. VI the conclusions are summarized.

II. MATERIAL AND FABRICATION

A description of the design and fabrication of the device used in this study was given by Seamons *et al.*[18] The UEHBL device was formed from molecular-beam epitaxy grown GaAs/AlGaAs double quantum well material (wafer EA1286) grown on the (100) surface of a GaAs substrate. A side profile diagram of the device after full processing is shown in Fig. 1(a). The top and bottom 18 nm GaAs quantum wells were separated by a 30 nm $Al_{0.9}Ga_{0.1}As$ barrier. Above the top quantum well is a 200 nm $Al_{0.3}Ga_{0.7}As$ cladding layer and a 60 nm Si-doped n^+ GaAs cap layer. Beneath the bottom quantum well is a 125 nm $Al_{0.3}Ga_{0.7}As$ cladding layer and a 310 nm growth superlattice. Beneath that is a 15 nm GaAs layer, which acts as the second etch stop during back-side processing and effectively becomes the cap layer. The first stop etch (not visible in diagram) is a 500 nm $Al_{0.55}Ga_{0.45}As$ layer and that is completely removed during processing.

Because our approach to electron-hole bilayers is to induce carriers with gate-generated electric fields, the processing for these devices is quite involved. The key steps are to define a Hall bar with an integrated top gate, define the n-type and p-type contacts, thin the structure for back-side processing, and apply a final metallization layer for both a back gate. An image of the final device is shown in Fig. 1(b), and the key steps are described below.

To process the UEHBL device an $\sim 6 \times 8$ mm^2 piece was cleaved from the wafer and mesa etched into the shape of a 200 μm wide Hall bar with five arms extending from it on each side. The only intentional dopants present in the material were in the n^+ cap layer that forms the top gate. These dopants do not provide the carriers to populate either of the quantum wells. Instead, electrons are pulled into the top quantum well from n-type NiGeAu self-aligned Ohmic contacts with the top gate.[19] A shallow annealing of PdGeAu metal was used to make Ohmic contact to the top gate [the right end of Fig. 1(b)]. In Fig. 1(b), the n-type contact and gate arms are outlined by the black dashed lines. The arms

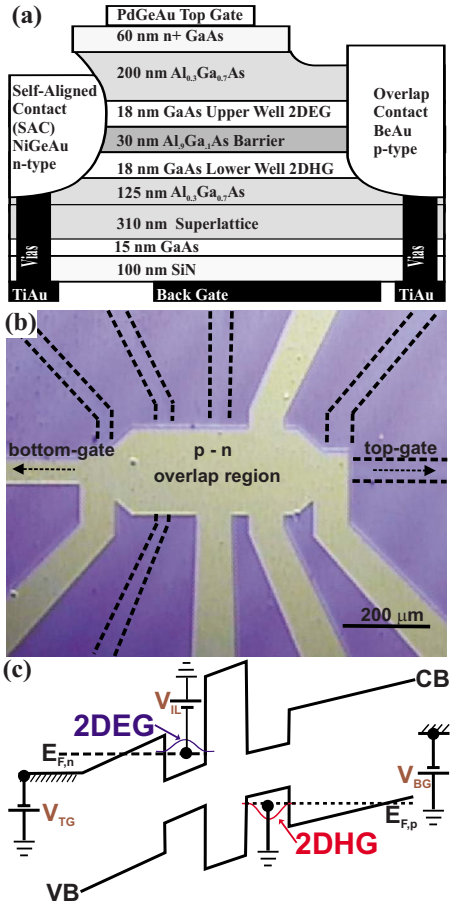

FIG. 1. (Color online) (a) Schematic of the UEHBL device. (b) Micrograph of the device. The top gate and n-type contacts are barely visible through the epimaterial and are outlined by black dashed lines. The back gate covering the Hall bar and p-type contact arms is the gold region. Top and bottom gate contact arms are located at the ends of the Hall bar; the actual contacts are not visible. (c) Schematic of the energy-band diagram depicting V_{TG}, V_{IL}, and V_{BG}.

are very difficult to see in the image because following back-side processing they end up beneath the epilayer, as will be discussed further below. The actual contact pads are not visible in the micrograph. These contacts served a dual role as reservoirs supplying electrons to the top quantum well and as the n-type Ohmic contacts for transport measurements on the 2DEG. At the ends of the remaining arms, AuBe p-type Ohmic contacts were formed.

The carriers in each quantum well were induced via external fields generated by gates on the top and bottom of the device, as depicted in Fig. 1(a). Each gate covers the central Hall bar region and extended along the entire length of half the arms in a geometry which allows for both longitudinal resistance R_{xx} and Hall resistance R_{xy} measurements in both wells independently. The gate contact pads were positioned at opposite ends of the long axis of the central Hall bar region [arms visible at right and left ends of Fig. 1(b)].

The patterning of the bottom gate of the device requires a procedure for thinning GaAs heterostructures called epoxy bond and stop etch (EBASE).[20] This technique entails epoxying the sample to a GaAs host substrate with the completely

processed top-side face down on the host substrate. The original GaAs substrate is removed down to the first stop-etch layer [$Al_{0.55}Ga_{0.45}As$, not shown in Fig. 1(a)] using a combination of lapping and selective etching of GaAs using citric acid. The first stop-etch layer is removed with an HF etch, which stops on the second stop-etch layer of GaAs. Once completed SiN was deposited over the entire mesa surface by plasma enhanced chemical vapor deposition and vias were etched through the heterostructure to contact the top electrical layers (n-type Ohmics, p-type Ohmics, and top gate). The back-gate metal, TiAu, was then deposited over the top of the SiN. The five p-type contact and the back-gate arms are clearly visible as gold regions in Fig. 1(b).

The back gate covers the central Hall bar region, the five p-type Ohmic contact arms, and a small portion of the p-type contacts. In this so-called *overlap* configuration, holes are pulled by the back gate into the bottom well from the p-type Ohmic contacts;[21] this is analogous to the aforementioned n-type Ohmic contacts' function. While both quantum wells are physically in contact with the n-type and p-type metal contacts, the gates and mesa configuration are such that only one type carrier is induced in each well. The positions of the contacts along the Hall bar were chosen to allow R_{xx} and R_{xy} measurements of both quantum wells independently; however, due to processing problems, only four contacts to each layer worked on this device and this led to measurements being made using the van der Pauw method.[22]

III. EXPERIMENT

A schematic of the energy-band diagram of the UEHBL during typical operation is given in Fig. 1(c). To simultaneously establish 2DEG and 2DHG in the UEHBL devices three different bias voltages, top-gate bias V_{TG}, bottom-gate bias V_{BG}, and interlayer bias V_{IL}, are necessarily used; all these voltages are referenced to ground. As depicted in Fig. 1(c), V_{TG}, V_{IL}, and V_{BG} predominantly adjust the electric fields across the 2DEG, barrier region, and 2DHG, respectively. During operation at least one p-type contact always remains grounded. The 2DEG is held at V_{IL}, which accounts for the difference in the electron and hole Fermi levels and ends up being slightly less (~1.43–1.45 meV) than the GaAs band-gap energy (~1.51 eV), due to the presence of other field sources, V_{TG}, V_{BG}, and the carriers in each well. Ideally, it is expected that n and p are controlled only by their nearest gate, the top and bottom gates, respectively, due to screening. However, as will be demonstrated below, changing the density in one well causes a small change in the density of the other well, requiring simultaneous adjustment of V_{TG} and V_{BG} for the mobility versus density measurements at constant V_{IL}. Additionally, the system is overdetermined (two densities and three voltage settings) so the same densities can be achieved at different gate voltage settings. Finally, with the 2DEG held at V_{IL} with respect to ground, all the circuitry connected to it must also be held at V_{IL}, necessitating the use of an isolation transformer to break the ground of the signal source. This also means that n is mainly proportional to $|V_{TG}-V_{IL}|$, while $p \propto |V_{BG}|$.

The n and p in the UEHBL were set by adjusting V_{TG}, V_{BG}, and V_{IL} and measured using low-magnetic-field R_{xy}

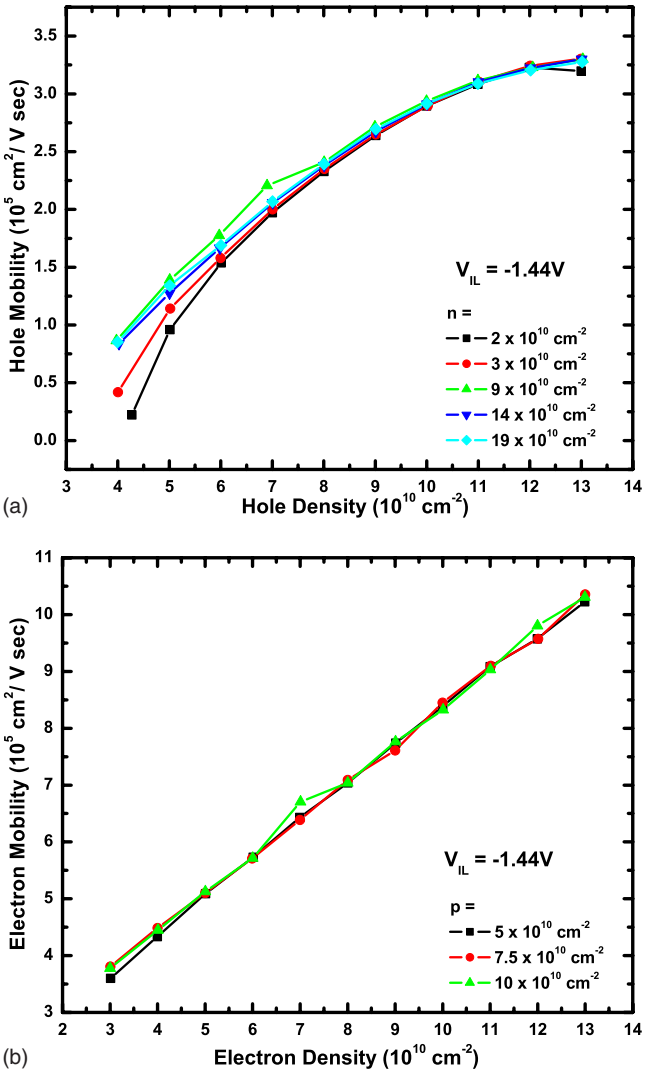

FIG. 2. (Color online) Mobilities (a) μ_p and (b) μ_n as a function of p and n, respectively, and the adjacent well density at $T=0.3$ K and $V_{IL}=-1.44$ V.

measurements. To characterize transport, the resistivity ρ was measured in each layer as a function of n and p, E_{IL}, and temperature T. The mobility in each layer was calculated from the resistivity and density according to $\mu_p = 1/pe\rho_p$ and $\mu_n = 1/ne\rho_n$. R_{xy} and ρ measurements were made by standard van der Pauw methods using low-frequency lock-in technique with separate 20 nA excitation currents in both layers. Coulomb drag measurements were used to estimate the change in d as V_{IL} changed. For these measurements a 10 nA current was driven in the 2DEG, while the induced voltage in the 2DHG was measured with a high-impedance detection circuit. The constant-temperature measurements were all taken at $T=0.3$ K in a He^3 refrigerator.

IV. RESULTS

To establish some basis for comparison, the mobility of each layer is plotted in Fig. 2 as a function of its density, n or p, at different densities in the adjacent layer with $V_{IL}=$

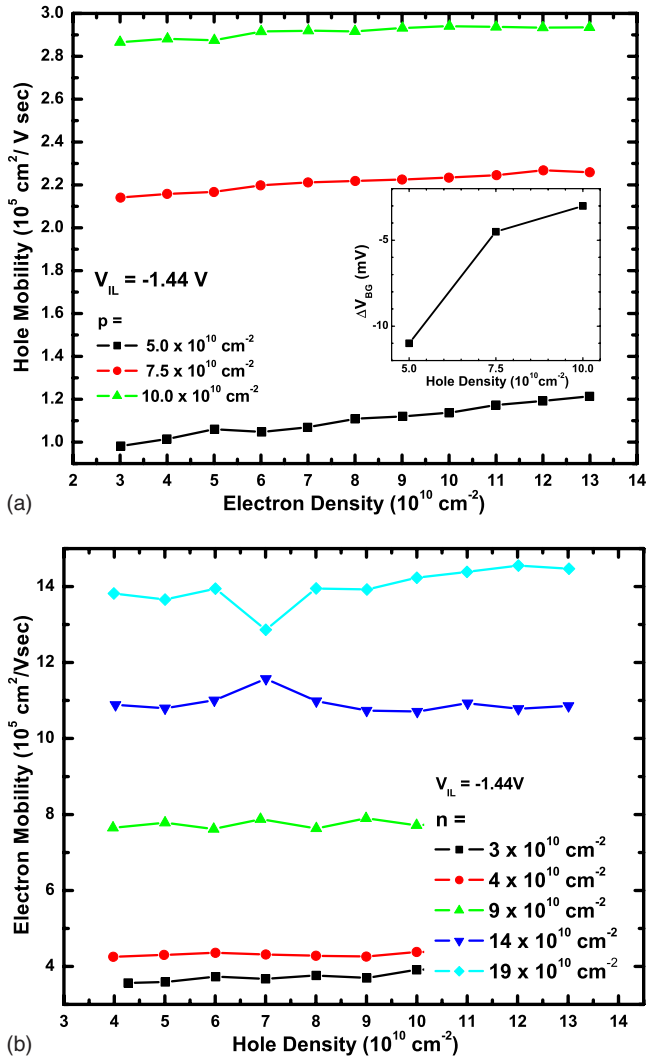

FIG. 3. (Color online) Mobilities (a) μ_p and (b) μ_n as a function of adjacent well carrier density, n and p, respectively, at $T=0.3$ K and $V_{IL}=-1.44$ V. The inset plot shows ΔV_{BG} as a function of p for the data in (a).

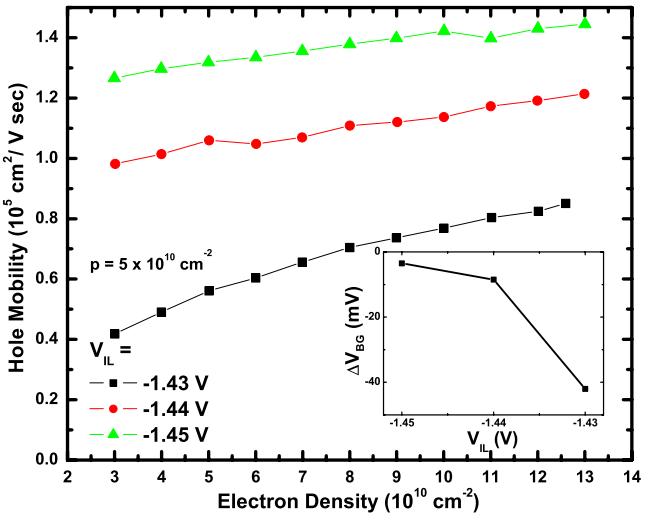

FIG. 4. (Color online) Mobility μ_p as a function of n for $V_{IL}=-1.43$ to -1.45 V and (inset) ΔV_{BG} as a function of V_{IL} at $T=0.3$ K.

-1.44 V. The resulting interlayer electric field E_{IL} is expected to be on the order of 10 kV/cm, far below the $\approx$500 kV/cm breakdown field of $Al_{0.9}Ga_{0.1}As$ in this temperature range.[23] In the traces of Fig. 2(a) an increase in hole mobility μ_p with increasing n is visible with a weakening dependence as p increases. In direct contrast, the traces in Fig. 2(b) of the electron mobility μ_n show minimal dependence on p, the density in its adjacent well. This mobility layer interdependence is more closely investigated in Fig. 3. First, these data show that the mobility in both layers increases with its density, as expected from Fig. 2. Second, the plots in Fig. 3(a) also show that there is a monotonically increasing relationship between the *hole* mobility μ_p and *electron* density n, the density in the adjacent well. At the lowest hole density, $p=5.0\times10^{10}$ cm^{-2}, $a\approx23\%$ change in μ_p was observed. As p was increased to 10.0×10^{10} cm^{-2} the percent change apparently becomes weaker, which is illustrated by the visible decrease in slope between the data sets. This decrease in slope corresponds to the data in Fig. 2(a), where the spread between plots was much larger for smaller p. The traces in Fig. 3(b) show that μ_n was roughly independent of p, confirming what was apparent in Fig. 2(b).

The inset plot of Fig. 3(a) shows the change in bottom-gate voltage ΔV_{BG} required to maintain a constant p while n was increased from 3.0×10^{10} to 13.0×10^{10} cm^{-2} using V_{TG} for each trace in the main plot. As previously mentioned, changing the density in one well often leads to a small change in the density of the other well, and thus, both gate voltages V_{TG} and V_{BG} must be simultaneously adjusted to set the densities. For all the measurements taken for this work, making V_{TG} less negative increased n, while making V_{BG} more negative increased p. According to the inset plot, as n was increased for each trace V_{BG} had to be made slightly more negative for p to remain constant. The increases in n for each trace thus result in small decreases in p since increasing V_{TG} (making V_{TG} less negative) to increase n required making V_{BG} more negative to keep p constant. Furthermore, the steepness of the slopes of each trace in Fig. 3(a) correlates with the magnitude of the change in V_{BG} in the inset plot; as $|V_{BG}|$ increases, the slope becomes steeper.

In Fig. 4 the same μ_p data at $p=5\times10^{10}$ cm^{-2} and $V_{IL}=-1.44$ V from Fig. 3(a) are plotted alongside similar measurements at $V_{IL}=-1.45$ and -1.43 V. The data in Fig. 4 were taken to examine the role of V_{IL} in determining μ_p, as changing V_{IL} was also expected to alter the 2DHG and 2DEG wave functions. With the 2DHG held at ground, making V_{IL}, the voltage dropped across the barrier and less negative pulled the 2DEG energy level down toward the 2DHG energy and, thereby, increased E_{IL}. Measurements of μ_n under similar conditions (not shown) were also taken but showed no discernable dependence on V_{IL}. The inset plot of Fig. 4 shows the ΔV_{BG} required to maintain constant p while increasing n from 3.0×10^{10} to 12.0×10^{10} cm^{-2} at each V_{IL}.

Based on the previous results in Fig. 3(a), the slopes of each data sets in Fig. 4 suggest, and the inset data confirm, that the largest ΔV_{BG} occurred at $V_{IL}=-1.43$ V since it has the steepest slope and that ΔV_{BG} increases with decreasing

V_{IL}. For fixed n, the traces also show an increase in μ_p as V_{IL} decreases. In this case, however, the increase in μ_p was accompanied by an increase in V_{BG} (making it less negative) as V_{IL} decreased. For example, at $n=3\times10^{10}$ cm^{-2} a $V_{BG}=-1.647$ V resulted for $V_{IL}=-1.43$ V, which was more negative than $V_{BG}=-1.5735$ V at $V_{IL}=-1.45$ V. This implies that changing V_{IL} also has a large impact on μ_p since a comparison of the slopes of the traces in Figs. 3(a) and 4 with the inset data shows that making V_{BG} less negative would typically be associated with a reduction in μ_p, not an enhancement.

V. DISCUSSION

A discussion of the mechanisms that might qualitatively describe the results in Sec. IV, the apparent increase in μ_p as n increased, the lack of similar magnitude changes in μ_n, and the changes in hole transport and Coulomb drag with V_{IL}, is given in the following. The analysis of the UEHBL is complicated by the bipolar nature of the device and the related use of three different voltages to control the carrier densities and the two different field-effect transistor (FET) structures used to generate them. These make it difficult to determine the exact shape of the confining potentials in the device; however, the action of the gates on the confining potentials and the wave-function shape can still be qualitatively described sufficient for one of these mechanisms to seem likelier than the other two.

Mobility is directly proportional to τ_p and inversely proportional to m_h^*; changes in either could lead to the behavior of μ_p above. One previously mentioned method for varying τ_p is via squeezing of the wave function. If scattering is limited by background impurity scattering in the well region then increased squeezing of the hole wave function would lead to an increase in μ_p. Squeezing is known to reduce background impurity scattering in undoped heterostructures in this density range ($<10^{11}$ cm^{-2}).[10,12] In the UEHBL, the hole wave-function squeezing would increase with increasing n because V_{BG}, which tilts the 2DHG confinement potential, was simultaneously decreased (made more negative) to maintain a constant p, as shown in the inset of Fig. 3(a). A Boltzmann transport calculation for the mobility-density data of a similar structure showed that transport in each layer was qualitatively consistent with scattering being dominated by a uniform background impurity density.[24] Finally, the decrease in steepness of the slopes of each data set in Fig. 3(a) as p was increased is also consistent with squeezing since the change in μ_p is proportional to $-\Delta V_{BG}$, which correspondingly drops in magnitude as p increased [see inset of Fig. 3(a)].

While qualitatively ΔV_{BG} would move the hole wave function in the right direction for squeezing to occur the question that arises is whether the effect was large enough to cause a change in μ_p. An analysis of calculations on a 2DEG in an undoped 100 nm wide quantum well showed that a $\Delta E\approx18$ kV/cm led to an increase in background impurity scattering time of $\Delta\tau\approx3\times10^{12}$ s at $n=1\times10^{11}$ cm^{-2}.[10] If background impurity scattering was completely limiting μ_n then this effect would change it by $\sim5.0\times10^3$ cm^2/V s. In comparison, the μ_p results in Fig. 3(a) show a $\Delta V_{BG}=3$ mV at $p=1\times10^{11}$ cm^{-2} which led to a $\Delta\mu_p\approx4\times10^4$ cm^2/V s. It is not clear how these results would change for the case of holes or for a smaller well; however, squeezing effect on mobility increases as density is reduced.[10]

A second question which arises is why similar magnitude changes were not visible in the μ_n results since V_{TG} was also varied as p increased. If background impurity scattering also limited the 2DEG mobility then the results in Fig. 3(b), that μ_n is roughly independent of p, imply that squeezing of the electron wave function was much weaker than squeezing of the hole wave function as density in the respective adjacent well increased. A direct comparison of the changes in the top and bottom gate voltages is invalidated by the device's asymmetry with regard to the cladding layer widths and relatively different gate leakages. The latter was a function of the type of gate and contact combinations for either 2D system [see Fig. 1(a)]. Thus, it is possible that changes to V_{TG} caused relatively smaller changes in the electron wave function compared with V_{BG}'s effect on the hole wave function.

The second means by which to alter mobility is by varying m^*. In GaAs/AlGaAs heterostructures, the conduction-band structure is parabolic and can be described by a constant m_n^*, while the valence-band structure is highly nonparabolic due to admixing of the heavy-hole and light-hole subbands and that leads to m_h^* being a function of several factors, such as p, the orientation of the grown surface, and the confining potential's height, width, and symmetry. Changes in m_h^* with p and well width W in (100) GaAs quantum wells were recently measured by Zu *et al.*[15] using cyclotron resonance. They showed that m_h^* increased as p increases for fixed W and as W increases for fixed p. In the results of Sec. IV above, however, μ_p increases as the *adjacent* well density n increased, while p and W were both held constant. Furthermore, from the traces in both Figs. 2(a) and 3(a), μ_p always increases as p increased, which means that any increase in m_h^* due to increasing p, as implied by the results of Zu *et al.*,[15] must have been weaker than the increases in scattering time from increased p. Finally, the change in m_h^* required for a $\Delta\mu_p\approx2\times10^4$ cm^2/V s, which, for example, was roughly the change observed at $p=5.0\times10^{10}$ cm^{-2} in Fig. 3(a), is roughly $0.06m_e$. Based on an analysis of the results of Zu *et al.*,[15] this would equate to either a $\Delta W\approx5$ nm or a $\Delta p\approx2.0\times11^{10}$ cm^{-2}, neither of which is expected.

Variation in m^* is also effectively possible via the Rashba effect, a spin-orbit interaction found in systems lacking inversion symmetry that leads to spin splitting of subbands in the absence of a magnetic field.[25,26] In such systems the moving carriers feel an effective magnetic field proportional to the vector product of the carrier's in-plane velocity and an electric field which is present because of the inversion asymmetry.[27,28] In a quantum well the application of a surface-gate bias provides a source of inversion asymmetry and the spin splitting can be varied using the surface gate.[29,30] In GaAs/AlGaAs heterostructures the smaller band mass and weaker spin-orbit couplings of the electrons lead to, for our purposes, negligible Rashba effect in the conduction band; in the valence band, however, measurable effects

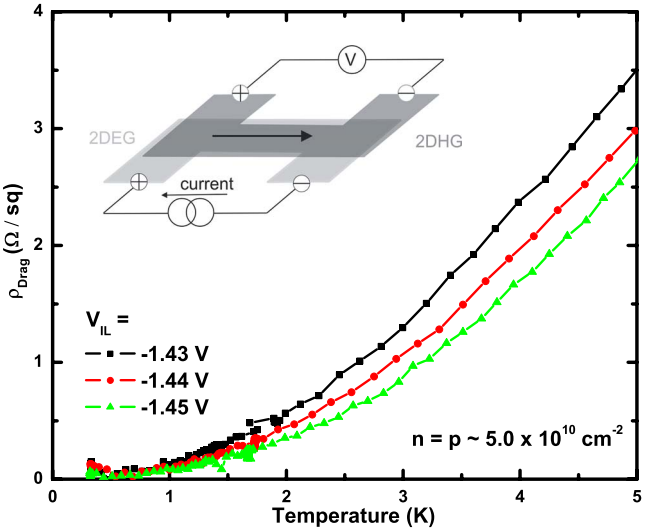

FIG. 5. (Color online) The hole drag resistivity ρ_{drag} as a function of T at matched density $n=p\sim 5.0\times 10^{10}$ cm^2 for various V_{IL} and (inset) schematic of the drag measurement.

are expected.[16,17,31] In the uppermost hole subband pair 2D heavy-hole and light-hole spin-split subbands result from the heavy-hole band.[32] By changing the spin splitting, the relative populations of the spin-split subbands can be varied and since these subbands have different m^* it is expected that the Rashba effect may thereby alter the effective mass of the system and correspondingly the mobility.

The confining potential for the 2DHG in the UEHBL was expected to be asymmetric due to V_{BG}, which generate the holes. Thus, making V_{BG} more negative was expected to increase the spin splitting of the 2DHG subbands. This would, in turn, increase the difference in relative populations of each spin-split hole subband, with a corresponding increase (decrease) in the population of the spin-split heavy (light) hole subband for constant p.[16] This change in relative populations should lead to an increase in m_h^* and, thereby, reduce μ_p. This type of behavior was not observed, however, as evidenced by the results in Fig. 3(a), where μ_p increases as n increased and simultaneously V_{BG} was made more negative so p remained constant. Thus, it appears that at least qualitatively the Rashba effect cannot account for the apparent layer interdependence of μ_p in the UEHBL data from Figs. 2 and 3. Furthermore, the observed changes in hole mobility were strongest at low density, while the Rashba effect is expected to occur mainly at larger k and vanish as $k\rightarrow 0$. Based on this analysis, it seems likely that squeezing of the hole wave function was the source of the apparent interlayer dependence manifest between μ_p and n.

To further elucidate the nature of the squeezing of the hole wave function in the UEHBL similar transport measurements, shown in Fig. 4, and Coulomb drag measurements, shown in Fig. 5, were then made at various V_{IL}. Making V_{IL} less (more) negative presumably increased (decreased) the field across the barrier since the 2DEG energy level was being pulled down toward (up away from) the 2DHG energy level, which was held at ground. Inspecting data from Fig. 4 it is apparent that squeezing also occurs at different V_{IL} and that V_{IL} significantly affects the relationship between μ_p and n and, thus, the amount of squeezing that occurs. Combined with the inset data of Fig. 4, these results are basically consistent with the previous discussion above; for each V_{IL} trace as n increased V_{BG} was made more negative and, presumably, this increased squeezing of the 2DHG wave function leads to an increase in μ_p. Considering these results more closely, however, another question arose, which is discussed in the following.

From the data in Fig. 4 and the related discussion in Sec. IV it appears that for constant p the presence of the weaker barrier field nearby caused μ_p to increase while having a negligible effect on μ_n. Furthermore, the process of making V_{IL} more negative was accompanied by an increase in V_{BG} to maintain a constant p. Based on the discussion above, the increase in V_{BG} would have reduced the squeezing effect and *decreased* μ_p. This crucial difference made the role played by V_{IL} less obvious and worthy of more investigation.

To further illustrate how the 2DHG was affected by changing the interlayer electric field and to provide an estimate of the e-h scattering contribution some Coulomb drag measurements, shown in Fig. 5, were taken as function of T at three different V_{IL} for matched density $n=p\sim 5.0\times 10^{10}$ cm^{-2}. At $T=0.3$ K a $\rho_{drag}\approx 0.1$ Ω/sq was equivalently measured for each V_{IL}. Using $\rho_{drag}=m_h^*/e^2p\tau_{h\rightarrow e}$ the time it takes for a hole to transfer its momentum to an electron is $\tau_{h\rightarrow e}\approx 313$ ns.[33] This was much longer than the hole scattering time τ_p, which varies from ~12.7 to 33.2 ps as V_{IL} decreases at $n=p=5\times 10^{10}$ cm^{-2} in Fig. 4, which eliminates e-h scattering as the dominant scattering mechanism.

The 2DHG Coulomb drag ρ_{drag} measurements in Fig. 5 also show that at a fixed $T>1.5$ K, ρ_{drag} decreased as V_{IL} was made more negative, which was expected, based on Boltzmann theory, to occur if d were to have increased.[33] To analyze the drag results more closely the ratio $[\rho_{drag}(A)/\rho_{drag}(B)]^{1/4}$ was determined, where A and B were the various V_{IL} and $A>B$. For a constant density this ratio is proportional to the ratio of interlayer separation $d(B)/d(A)$ at each V_{IL}. From the ratio calculation, the decrease of $\Delta V_{IL}=-10$ mV led to an increase $\Delta d\approx 5\%$. For the nominally expected separation $d=38$ nm, where the 2DEG and 2DHG wave functions would be located in the center of the wells, this change equates to roughly 1.9 nm. Intuitively, the increase in d makes sense; the strength of the actual electric field between the 2DEG and 2DHG is primarily due to V_{IL} and when the field is weaker than the charges it would be expected to be further apart from each other. Most importantly, however, this increase in d as V_{IL} decreased suggests the hole wave function moved away from the 2DEG and closer to the edge of the confinement potential where squeezing presumably occurs. Thus, making V_{IL} more negative also qualitatively suggests an increase in squeezing and, therefore, a commensurate increase in μ_p.

VI. CONCLUSION

The layer interdependence of low-temperature transport in a 30 nm barrier UEHBL device was investigated. An increase in μ_p with increasing n was observed at various p,

while minimal change in μ_n with increasing p was observed at any n. The former was accompanied by a simultaneous decrease in V_{BG} (made more negative) to maintain constant p while n was increased, which was expected to have changed the 2DHG confinement potential. Similar μ_p versus n results were seen at three different V_{IL}. Making V_{IL} more negative was also observed to increase both μ_p and d. A $\Delta d \approx 5\%$ increase with $\Delta V_{IL} = -10$ mV was determined by measurements of $\rho_{drag}(T)$. The μ_p results, which manifested an apparent layer interdependence on adjacent layer density n, were then discussed with regard to the following mechanisms related to varying mobility: wave-function squeezing, anisotropic band structure, and spin splitting of the subbands due to the Rashba effect. Based on the analysis it appears that hole wave-function squeezing was, at least qualitatively, the best candidate as the source of the apparent layer interdependence. Bolstering this argument, the increase in d, suggested by the 2DHG drag measurements, as V_{IL} was made more negative was also consistent with squeezing of the hole wave function modulating μ_p.

ACKNOWLEDGMENTS

The authors acknowledge Denise Tibbets for her technical assistance. The authors also wish to thank S. Das Sarma and E. H. Hwang for their helpful discussions of the related theory. This work has been supported by the Division of Materials Sciences and Engineering, Office of Basic Energy Sciences, U.S. Department of Energy. Sandia is a multiprogram laboratory operated by Sandia Corporation, a Lockheed Martin Co., for the United States Department of Energy under Contract No. DE-AC04-94AL85000.

*Also at Physics and Astronomy Department, University of New Mexico; cpmorat@sandia.gov

[1] S. I. Shevchenko, Sov. J. Low Temp. Phys.0031-7918 **2**, 251 (1976).
[2] Y. E. Lozovik and V. I. Yudson, Solid State Commun. **19**, 391 (1976).
[3] L. V. Butov, J. Phys.: Condens. Matter **16**, R1577 (2004).
[4] J. A. Seamons, C. P. Morath, J. L. Reno, and M. P. Lilly, arXiv:0808.1322 (unpublished).
[5] T. Ando, A. B. Fowler, and F. Stern, Rev. Mod. Phys. **54**, 437 (1982).
[6] W. Walukiewicz, H. E. Ruda, J. Lagowski, and H. C. Gatos, Phys. Rev. B **30**, 4571 (1984).
[7] K. Hirakawa, H. Sakaki, and J. Yoshino, Phys. Rev. Lett. **54**, 1279 (1985).
[8] A. Kurobe, J. E. F. Frost, M. P. Grinshaw, D. A. Ritchie, G. A. C. Jones, and M. Pepper, Appl. Phys. Lett. **62**, 2522 (1993).
[9] A. Kurobe, I. Castleton, E. Linfield, M. Grimshaw, K. Brown, D. Ritchie, G. Jones, and M. Pepper, Semicond. Sci. Technol. **9**, 1744 (1994).
[10] A. Kurobe, Semicond. Sci. Technol. **8**, 742 (1993).
[11] Y. Markus, U. Meirav, H. Shtrikman, and B. Laikhtman, Semicond. Sci. Technol. **9**, 1297 (1994).
[12] E. K. Pettersen, D. A. Williams, and H. Ahmed, Semicond. Sci. Technol. **11**, 1151 (1996).
[13] S. Das Sarma, M. P. Lilly, E. H. Hwang, L. N. Pfeiffer, K. W. West, and J. L. Reno, Phys. Rev. Lett. **94**, 136401 (2005).
[14] M. J. Manfra, E. H. Hwang, S. Das Sarma, L. N. Pfeiffer, K. W. West, and A. M. Sergent, Phys. Rev. Lett. **99**, 236402 (2007).
[15] H. Zhu, K. Lai, D. C. Tsui, S. P. Bayrakci, N. P. Ong, M. Manfra, L. Pfeiffer, and K. West, Solid State Commun. **141**, 510 (2007).
[16] J. P. Lu, J. B. Yau, S. P. Shukla, M. Shayegan, L. Wissinger, U. Rossler, and R. Winkler, Phys. Rev. Lett. **81**, 1282 (1998).
[17] S. J. Papadakis, E. P. De Poortere, and M. Shayegan, Phys. Rev. B **62**, 15375 (2000).
[18] J. A. Seamons, D. R. Tibbetts, J. L. Reno, and M. P. Lilly, Appl. Phys. Lett. **90**, 052103 (2007).
[19] B. E. Kane, L. N. Pfeiffer, K. W. West, and C. K. Harnett, Appl. Phys. Lett. **63**, 2132 (1993).
[20] M. V. Weckwerth, J. A. Simmons, N. E. Harff, M. E. Sherwin, M. A. Blount, W. E. Baca, and H. C. Chui, Superlattices Microstruct. **20**, 561 (1996).
[21] R. L. Willett, L. N. Pfeiffer, and K. W. West, Appl. Phys. Lett. **89**, 242107 (2006).
[22] L. J. van der Pauw, Philips Res. Rep. **13**, 1 (1958).
[23] F. Ma, G. Karve, X. Zheng, X. Sun, A. Holmes, and J. Campbell, Appl. Phys. Lett. **81**, 1908 (2002).
[24] E. H. Hwang and S. Das Sarma, Phys. Rev. B **78**, 075430 (2008).
[25] Y. A. Bychkov and E. I. Rashba, J. Phys. C **17**, 6039 (1984).
[26] U. Rössler, F. Malcher, and G. Lommer, Springer Series in Solid-State Sciences (Springer-Verlag, Berlin, 1989), Vol. 87.
[27] H. L. Stormer, Z. Schlesinger, A. Chang, D. C. Tsui, A. C. Gossard, and W. Wiegmann, Phys. Rev. Lett. **51**, 126 (1983).
[28] J. P. Eisenstein, H. L. Störmer, V. Narayanamurti, A. C. Gossard, and W. Wiegmann, Phys. Rev. Lett. **53**, 2579 (1984).
[29] M. Schultz, F. Heinrichs, U. Merkt, T. Colin, T. Skauli, and S. Lovold, Semicond. Sci. Technol. **11**, 1168 (1996).
[30] J. Nitta, T. Akazaki, H. Takayanagi, and T. Enoki, Phys. Rev. Lett. **78**, 1335 (1997).
[31] S. Papadakis, E. P. De Poortere, H. C. Manoharan, M. Shayegan, and R. Winkler, Science **283**, 2056 (1999).
[32] U. Ekenberg and M. Altarelli, Phys. Rev. B **32**, 3712 (1985).
[33] T. J. Gramila, J. P. Eisenstein, A. H. MacDonald, L. N. Pfeiffer, and K. W. West, Phys. Rev. Lett. **66**, 1216 (1991).